DOI:10.7598/cst2017.1415
ISSN:2278-3458

Chemical Science Transactions
2017, **6(4),** 545-560

RESEARCH ARTICLE

Studies on Benzylidene/Dibenzylidene Thiosemicarbazide Complexes of Zn(II), Cd(II) and Hg(II): Single Source Precursor in Pyrolytic Synthesis of Quantum Dots

S. N. SHUKLA[*], P. GAUR[1], N. RAI[1], R. MEHROTRA[2], B. CHAURASIA[1], J. P. GUPTA[1] and B. K. SINHA[3]

[1]Coordination Chemistry Research Lab, Department of Chemistry, Govt. Science College, Jabalpur (MP) 482001, India

[2]Instituto de Quimica Rosario Area Inorganica Facultad de Cs. Bioqumicas y Farmaceuticas Universidad Nacional de Rosario Suipacha 531 S2002LRK Rosario, Argentina

[3]Department of Physics, Institute for Excellence in Higher Education (IEHE), Bhopal (M. P.) 462012, India

sns1963_1@rediffmail.com

Received 4 June 2017 / Accepted 30 June 2017

Abstract: Twelve complexes of Zn(II), Cd(II) and Hg(II) with two sulphur containing Schiff base ligands, 1-benzylidenethiosemicarbazide (1-BTC) and 1,4-dibenzylidenethiosemicarbazide (1,4-DBTC) in 1:1 and 1:2 ratio have been synthesized. Complexes were characterized by molar conductance, elemental analyses, FT-IR, ^{1}H NMR and FAB/ESI-mass. The complexes were used as a single source precursor for the synthesis of ZnS/CdS/HgS nanoparticles by their pyrolytic decomposition in the presence of different surfactants. The precursor : surfactant ratio and temperature plays important role in determining the size of the nanoparticles. The size and morphology of nanoparticles has been ascertained by UV-Vis spectroscopy, XRD measurements and transmission electron microscopy (TEM). Schiff bases, complexes and nanoparticles were screened for antibacterial activity and MIC values against *E. coli*. The complexes were found more potent than the corresponding Schiff bases and nanoparticles.

Keywords: Schiff base complexes, Metal sulphide nanoparticles, Benzylidenethiosemicarbazide, Thermal decomposition, X-ray diffraction, Transmission electron microscopy

Introduction

In the last few years, researchers have shown interest in smart material with tunable properties by altering the nanostructure size, shape and chemical composition and have

developed reproducible strategies to make nanostructures of desired properties[1-3]. It has been already proved that by controlling the size of the particle and manipulating surface structures of the semiconductor materials, the electronic, magnetic, mechanical and chemical properties can be modified to suit a wide range of device application in many fields[4].

Thermal decomposition (*i.e*. thermolysis or pyrolysis) of complex precursors is one of the representative methods to obtain monodisperse nanoparticles[5], which allowed easier and simpler control of the shapes and sizes of nanoparticles than other methods.

Fluorescent semiconductor nanocrystals are a kind of quantum dots (QDs), which are of considerable interest and under intensive research as biological labels either *in vitro* or *in vivo*, not only because of their bright, photostable fluorescence but also because of the broad excitation spectrum and narrow, size-controlled emission, which allows multi-color imaging[6]. CdS nanoparticles functionalized colloidal carbon particles which were further used for the ultrasensitive electrochemical determination of thrombin[7]. Shiohara *et al.,* have investigated the cytotoxic effects of ZnS particles of different size on three different cell types and claims that for ZnS particles the main source of cytotoxicity is not their cadmium content but rather their interaction of the particle surface with the cells[8].

Therefore, in anticipation of an interesting chemistry and biological activity, we have synthesized two benzylidene/dibenzylidene thiosemicarbazide, Schiff bases and their complexes with Cd(II), Zn(II) and Hg(II) in different molar ratio and characterized them by spectroscopic methods. These complexes were further used as a single source precursor for the thermal/pyrolytic synthesis of metal sulphide nanoparticles. The actual aim of this work is to corroborate how Schiff base metal derivative could be used as single source precursor for the thermal pyrolytic synthesis of metal sulphide nanoparticles and to study and compare the antibacterial activity of the Schiff bases, complexes and nanoparticles synthesized.

Experimental

All the chemicals and solvents were used of A.R. grade. Mercury(II) chloride, cadmium(II) chloride, thiosemicarbazide, benzaldehyde, trioctylphosphine oxide (All E. Merck), HDA (Aldrich), zinc(II) chloride (CDH) were used as received. Rest of the experimental procedure is same as discussed earlier[9].

Synthesis of ligands

Synthesis of 1-benzylidene thiosemicarbazide (1-BTC)

This ligand was prepared according to literature procedure[10-14]. Thiosemicarbazide (4.557 g, 0.05 mol) was dissolved into 25 mL methanol in a two neck flask. Benzaldehyde (5.00 mL, 0.05 mol) mixed into 25 mL of methanol was added to above reaction mixture. The reaction mixture was kept under reflux for 25 h in an inert atmosphere and the concentrated solution was poured into ice-cold water. A white precipitate was obtained which was filtered and vacuum dried at room temperature. Yield: 7.360 g (84.028%); Mp = 160-162 °C; Found: C, 52.56; H, 5.12; N, 22.50; S, 17.80. $C_8H_9N_3S$ (Mτ = 179.24). Requires: C, 53.60; H, 5.06; N, 23.44; S, 17.88. Selected Infrared absorption (KBr, cm^{-1}): $\nu(N\text{-}H)_{asym}$, 3423m; $\nu(N\text{-}H)_{sym,}$ 3257m; $\delta(NH_2)+\nu(CH=N)$, 1591s; 1543m; ν(C=S), 815w. ^1H NMR spectra (300MHz, δ, MeOD): $\delta(NH_2)$, 3.305(s, 2H); δ(NH), 3.315-3.310(s, H); δ(Ar-H), 7.757-7.725(m, 2H); 7.413-7.392(m, 3H); δ(HC=N), 7.893(s, H). FAB-Mass $[M+H]^+$ *m/z* = 180.

Synthesis of 1, 4-dibenzylidene thiosemicarbazide (1,4-DBTC)

Thiosemicarbazide (4.557 g, 0.05 mol) was dissolved into 50 mL methanol in a two neck flask. Benzaldehyde (10.16 mL, 0.10 mol) mixed into 50 mL of methanol was added into above reaction mixture. The reaction mixture was refluxed for 25 h in an inert atmosphere and the concentrated solution was poured into ice-cold water. A white precipitate was obtained, which was filtered, recrystallized from methanol: water, 1:1 (v/v) solvent mixture and vacuum dried at room temperature. Yield: 10.59 g (81.63%), Mp=149-153 °C. Found: C, 67.42; H, 4.80; N, 15.57; S, 11.82; $C_{15}H_{13}N_3S$ (Mτ=267.34) Requires: C, 67.30; H, 4.90; N, 15.71; S, 11.99. Selected Infrared absorption (KBr, cm^{-1}): $\nu(N\text{-}H)_{asym}$, 3423m; $\nu(N\text{-}H)_{sym,}$ 3257m; $\delta(NH_2)+\nu(CH=N)$, 1591s; 1543m; ν(C=S), 800w. ^1H NMR Spectra (300MHz, δ, MeOD): δ(N-H), 3.314-3.310(s, H); δ(Ar-H), 7.760-7.729(qt, 4H); 7.415-7.394(t, 6H); δ(HC=N), 7.985(s, 2H). FAB-Mass $[M+H]^+$ *m/z* = 268.

Synthesis of complexes with the ligand, 1-BTC

*Synthesis of [M(1-BTC)Cl_2], Complex **1, 3** and **5***

Metal chloride (M = Zn^{2+}, Cd^{2+} and Hg^{2+}), (0.001 mol) was dissolved in 10 mL of methanol in a two neck flask. The ligand 1-BTC (0.179 g, 0.001 mol) dissolved in 10 mL of methanol, was added to the above solution and stirred for 2-3 h. A dirty white (Complex **1**)/ white (Complex **3**) / creamy white (Complex **5**) precipitate was obtained after 7-8 h reflux, which was filtered, dried at room temperature and recrystallized from methanol:acetone: chloroform, 1: 2: 2 (v/v) solvent mixture.

*[Zn(C_6H_5CH=N-NH-CS-NH_2)Cl_2] Complex **1***

Yield: 0.285 g (90.4%). Mp=148-152 °C; found: C, 30.2; H, 2.7; N, 12.76; S, 9.8. $C_8H_9N_3SCl_2Zn$ (Mτ=315.53). Requires: C, 30.45; H, 2.87; N, 13.31; S, 10.16. Λ_m at 25 °C ($\Omega^{-1}cm^2mol^{-1}$): 12.5 in MeOH. Selected Infrared absorption (KBr, cm^{-1}): $\nu(N\text{-}H)_{asym}$, 3442m; $\nu(N\text{-}H)_{sym}$, 3293m; $\delta(NH_2)+\nu(CH=N)$, 1611s, 1546m; ν(C=S), 768w. ^1H NMR Spectra (300MHz, δ, MeOD): $\delta(NH_2)$, 3.308(m, 2H); δ(NH), 3.316-3.312(s, H); δ(Ar-H), 7.771-7.742(m, 2H), 7.429-7.376(m, 3H); δ(HC=N), 8.162(s, H). FAB-Mass *m/z*: $[ZnCl]^+$ = 100.8; $[C_8H_9ZnClN_3S]^+$ = 280; $[C_8H_9ZnCl_2N_3S+H^+]^+$ = 316.54.

*[Cd(C_6H_5CH=N-NH-CS-NH_2)Cl_2] Complex **3***

Yield: 0.265 g (73.2%). Mp^d=250-255 °C; Found: C, 26.42; H, 2.40; N, 10.50; S, 8.66. $C_8H_9N_3SCl_2Cd$ (Mτ=362.55). Requires: C, 26.50; H, 2.50; N, 11.58; S, 8.84. Λ_m at 25 °C (Ω^{-1} cm^2mol^{-1}): 18.2 in DMSO. Selected Infrared absorption (KBr, cm^{-1}): $\nu(N\text{-}H)_{asym}$, 3432m, $\nu(N\text{-}H)_{sym}$, 3283m; $\delta(NH_2)+\nu(CH=N)$, 1606s; 1556m; ν(C=S), 780w. ^1H NMR Spectra (300, δ, MeOD): $\delta(NH_2)$, 3.309(m, 2H); δ(NH), 3.322-3.314(s, H); δ(Ar-H), 7.783-7.742(m, 2H); 7.401-7.391(m, 3H); δ(HC=N), 8.204(s, H). FAB-Mass *m/z*: $[CdCl]^+$ = 148; $C_8H_9CdClN_3S]^+$ = 327; $[C_8H_9CdCl_2N_3S+H^+]^+$ = 363.56.

*[Hg(C_6H_5CH=N-NH-CS-NH_2)Cl_2] Complex **5***

Yield: 0.415 g (92.2%). Mp=180 °C; Found: C, 20.47; H, 1.93; N, 9.27; S, 6.23. $C_8H_9N_3SCl_2Hg$ (Mτ=494.53). Requires: C, 21.31; H, 2.01; N, 9.32; S, 7.11. Λ_m at 25 °C (Ω^{-1} cm^2mol^{-1}): 32.5 in DMSO. Selected Infrared absorption (KBr, cm^{-1}): $\nu(N\text{-}H)_{asym}$, 3381m, $\nu(N\text{-}H)_{sym}$, 3263m; $\delta(NH_2)+\nu(CH=N)$, 1602s; 1566m; ν(C=S), 779w. ^1H NMR Spectra (300MHz, δ, MeOD): $\delta(NH_2)$, 3.316(m, 2H), δ(NH), 3.326-3.319(s, H); δ(Ar-H), 7.775-7.710(m, 2H), 7.407-7.388(m, 3H), δ(HC=N), 8.120(s, H). FAB-Mass *m/z*: $[HgCl]^+$ = 237; $[C_8H_9HgClN_3S]^+$ = 416; $[C_8H_9HgCl_2N_3S+H^+]^+$ = 451.

*Synthesis of [M(1-BTC)$_2$]Cl$_2$, Complex **2, 4** and **6***

Metal chloride (M = Zn^{2+}, Cd^{2+} and Hg^{2+}), (0.001 mol) was dissolved in 10 mL of methanol in a two neck flask. The ligand 1-BTC (0.358 g, 0.002 mol) dissolved in 20 mL of methanol was added to the above solution. This reaction mixture was stirred for 2-3 h and then refluxed for 10-12 h. A white/dirty white/creamy white precipitate was obtained which was filtered, dried at room temperature and recrystallized from methanol: ethanol: acetone, 1:2:3 (v/v) solvent mixtures.

*[Zn(C$_6$H$_5$CH=N-NH-CS-NH$_2$)$_2$]Cl$_2$ Complex **2***

Yield: 0.460 g (93.4%). Mp^d=185 °C; found: C, 37.79; H, 3.62; N, 15.89; S, 12.62. $C_{16}H_{18}N_6S_2Cl_2Zn$ (Mτ=494.53). Requires: C, 38.84; H, 3.66; N, 16.98; S, 12.96. Λ_m at 25 °C ($\Omega^{-1}cm^2mol^{-1}$): 162.5 in MeOH. Selected Infrared absorption (KBr, cm^{-1}): ν(N-H)$_{asym}$, 3344m, ν(N-H)$_{sym}$, 3288m; δ(NH$_2$)+ν(CH=N), 1597s; 1560m; ν(C=S), 772w. ^{1}H NMR Spectra (300MHz, δ, MeOD): δ(NH$_2$), 3.306(m, 4H); δ(NH), 3.319-311(s, 2H); δ(Ar-H), 7.770-7.747(m, 4H); 7.425-7.376(m, 6H); δ(CH), 8.034(s, 2H). FAB-Mass *m/z*: $[C_{16}H_{18}N_6S_2Zn]^{++}$ = 422.03; $[C_{10}H_{11}N_5S_2Zn]^{++}$ = 328.97; $[C_9H_{12}N_5S_2Zn]^{++}$ = 317.98; $[C_9H_{11}N_4S_2Zn]^{++}$ = 302.97; $[C_4H_8N_6S_2Zn]^{++}$ = 267.95; $[C_8H_9N_3SZn]^{++}$ = 242.98; $[C_8H_9N_3S]^{++}$ = 179.05; $[C_7H_7N_2]^{++}$ = 119.06; $[C_7H_6N]^{++}$ = 104.05.

*[Cd(C$_6$H$_5$CH=N-NH-CS-NH$_2$)$_2$]Cl$_2$ Complex **4***

Yield: 0.208 g (38.4%). Mp^d=230 °C; Found: C, 35.33; H, 3.13; N, 14.78; S, 10.93. $C_{16}H_{18}N_6S_2Cl_2Cd$ (Mτ=541.77). Requires: C, 35.46; H, 3.34; N, 15.51; S, 11.83. Λ_m at 25 °C ($\Omega^{-1}cm^2mol^{-1}$): 169.2 in DMSO. Selected Infrared absorption (KBr, cm^{-1}): ν(N-H)$_{asym}$, 3432m; ν(N-H)$_{sym}$, 3283m; δ(NH$_2$)+ν(CH=N), 1606s, 1561m; ν(C=S), 770w. ^{1}H NMR Spectra (300MHz, δ, MeOD): δ(NH$_2$), 3.312 (m, 4H); δ(NH), 3.330-3.324(s, 2H); δ(Ar-H), 7.773-7.718(m, 4H); 7.414-7.393(m, 6H); δ(HC=N), 8.018(s, 2H); FAB-Mass *m/z*: $[C_{16}H_{18}CdN_6S_2]^{++}$ = 472.01; $[C_{10}H_{11}CdN_5S_2]^{+}$ = 378.95; $[C_9H_{12}N_5S_2Cd]^{++}$ = 367.96; $[C_9H_{11}N_4S_2Cd]^{++}$ = 352.95; $[C_4H_8CdN_6S_2]^{++}$ = 317.93; $[C_8H_9CdN_3S]^{++}$ = 292.96; $[C_8H_9N_3S]^{++}$ = 179.05; $[C_7H_7N_2]^{++}$ = 119.06; $[C_7H_6N]^{++}$ = 104.05.

*[Hg(C$_6$H$_5$CH=N-NH-CS-NH$_2$)$_2$]Cl$_2$ Complex **6***

Yield: 0.590 g (93.7%). Mp^d=185 °C; C, 29.65; H, 2.11; N, 12.57; S, 9.83. $C_{16}H_{18}N_6S_2C_{l2}Hg$ (Mτ=629.98). Requires: C, 30.50; H, 2.87; N, 13.34; S, 10.17. Λ_m at 25 °C ($\Omega^{-1}cm^2mol^{-1}$): 160.2 in DMSO. Selected Infrared absorption (KBr, cm^{-1}): ν(N-H)$_{asym}$, 3435m, ν(N-H)$_{sym}$, 3261m; δ(NH$_2$)+ν(CH=N), 1599s, 1556, ν(C=S)m, 776w. ^{1}H NMR Spectra (300MHz, δ, MeOD): δ(NH$_2$), 3.301(m, 4H); δ(NH), 3.321-314(s, 2H); δ(Ar-H), 7.781-7.736(m, 4H); 7.413-7.394(m, 6H), δ(HC=N), 8.234(s, 2H). FAB-Mass (*m/z*): $[C_{16}H_{18}N_6S_2Hg]^{++}$ = 560.07; $[C_{10}H_{11}N_5S_2Hg]^{++}$ = 467.02; $[C_9H_{12}N_5S_2Hg]^{++}$ = 456.02; $[C_4H_8N_6S_2Hg]^{++}$ = 406.00; $[C_8H_9N_3SHg]^{++}$ = 381.02; $[C_8H_9N_3S]^{++}$ = 179.05; $[C_9H_{11}N_4S_2Hg]^{++}$ = 441.01; $[C_7H_7N_2]^{++}$ = 119.06; $[C_7H_6N]^{++}$ = 104.05.

Synthesis of complexes with the ligand, 1,4-DBTC

*Synthesis of [M(1,4-DBTC)Cl$_2$], Complex **7, 9** and **11***

Metal chloride (M = Zn^{2+}, Cd^{2+} and Hg^{2+}), (0.001 mol) was dissolved in 10 mL of methanol in a two neck flask. The ligand 1,4-DBTC (0.267 g, 0.001 mol) dissolved in 10 mL of methanol was added to the above solution and stirred for 2-3 h. A white/dirty white/creamy white precipitate was obtained after 7-8 h reflux, which was filtered, dried at room temperature and recrystallized from methanol: acetone: chloroform, 1: 2: 2,(v/v) solvent mixture.

*[Zn(C_6H_5CH=N-NH-CS-N=HC-C_6H_5)Cl_2] Complex **7***

Yield: 0.383 g (95.03%). Mp^d=188 °C; Found: C, 44.59; H, 2.78; N, 10.33; S, 6.92. $C_{15}H_{13}N_3SCl_2Zn$ (Mτ=403.63). Requires: C, 44.63; H, 3.24; N, 10.41; S, 7.94. Λ_m at 25 °C ($\Omega^{-1}cm^2mol^{-1}$): 26.7 in MeOH. Selected Infrared absorption (KBr, cm^{-1}): ν(N-H)$_{asym}$, 3429m; ν(N-H)$_{sym}$, 3284m; δ(NH_2)+ν(CH=N), 1595s; 1545m; ν(C=S) 793w. ^{1}H NMR Spectra (300MHz, δ, MeOD): δ(NH), 2.861(s, H); δ(Ar-H), 7.771-7.743(m, 4H); 7.432-7.416(m, 6H); δ(HC=N), 8.013(s, 2H). FAB-Mass (*m/z*): $[ZnCl]^+$=100.8; $[C_{15}H_{13}ClN_3SZn]^+$ = 366; $[C_{15}H_{13}Cl_2N_3SZn+H^+]^+$ = 402.

*[Cd(C_6H_5CH=N-NH-CS-N=HC-C_6H_5)Cl_2] Complex **9***

Yield: 0.260 g (57.64%). Mp^d=230-235 °C; Found: C, 37.66; H, 1.87; N, 8.97; S, 6.23. $C_{15}H_{13}N_3SCl_2Cd$ (Mτ=450.65). Requires: C, 39.97; H, 2.90; N, 9.32; S, 7.11. Λ_m at 25 °C ($\Omega^{-1}cm^2mol^{-1}$): 10.8 in DMSO. Selected Infrared absorption (KBr, cm^{-1}): ν(N-H)$_{asym}$, 3433m; ν(N-H)$_{sym}$, 3185m; δ(NH_2)+ν(CH=N), 1603s; 1562m; ν(C=S), 810w. ^{1}H NMR Spectra (300MHz, δ, MeOD): δ(NH), 2.892(s, H); δ(Ar-H), 7.681-7.626(m, 4H); 7.405-7.387(m, 6H); δ(HC=N), 8.108(s, 2H). FAB-Mass (*m/z*): $[CdCl]^+$=148; $[C_{15}H_{13}ClN_3SCd]^+$ = 416; $[C_{15}H_{13}Cl_2N_3SCd+H^+]^+$ = 452.

*[Hg(C_6H_5CH=N-NH-CS-N=HC-C_6H_5)Cl_2] Complex **11***

Yield: 0.492 g (91.4%). Mp=176 °C; Found: C, 32.68; H, 2.13; N, 7.21; S, 4.57. $C_{15}H_{13}N_3SCl_2Hg$ (Mτ=538.84). Requires: C, 33.43; H, 2.43; N, 7.79; S, 5.95. Λ_m at 25 °C ($\Omega^{-1}cm^2mol^{-1}$): 29.5 in DMSO. Selected Infrared absorption (KBr, cm^{-1}): ν(N-H)$_{asym}$, 3284m; ν(N-H)$_{sym}$, 3176m; δ(NH_2)+ν(CH=N), 1600s; 1556m; ν(C=S), 806w. ^{1}H NMR Spectra (300MHz, δ, MeOD): δ(NH), 2.829(s, H); δ(Ar-H), 7.760-7.731(m, 4H); 7.423-7.410(m, 6H); δ(HC=N), 8.056(s, 2H). FAB-Mass (*m/z*): $[HgCl]^+$=237; $[C_{15}H_{13}ClN_3SHg]^+$ = 504; $[C_{15}H_{13}Cl_2N_3SHg+H^+]^+$ = 540.

*Synthesis of [M(1,4-DBTC)$_2$] Cl_2, Complex **8, 10, 12***

Metal chloride (M = Zn^{2+}, Cd^{2+} and Hg^{2+}), (0.001 mol) was dissolved in 10 mL of methanol in a two neck flask. The ligand 1,4-DBTC (0.535 g, 0.002 mol) dissolved in 20 mL of methanol was added to the above solution. This reaction mixture was stirred for 4-5 h and then refluxed for 12-14 h. A dirty white/white/creamy white precipitate was obtained which was filtered, dried at room temperature and recrystallized from methanol: ethanol: chloroform, 1: 2: 3 (v/v) solvent mixture.

*[Zn(C_6H_5CH=N-NH-CS-N=HC-C_6H_5)$_2$]Cl_2 Complex **8***

Yield: 0.595 g (88.80%). Mp=158-160 °C; Found: C, 52.39; H, 3.22; N, 11.66; S, 8.92. $C_{30}H_{26}N_6S_2Cl_2Zn$ (Mτ=670.98). Requires: C, 53.70; H, 3.90; N, 12.52; S, 9.74. Δ_m at 25 °C ($\Omega^{-1}cm^2mol^{-1}$): 172.9 in MeOH. Selected Infrared absorption (KBr, cm^{-1}): ν(N-H)$_{asym}$, 3417m; ν(N-H)$_{sym}$, 3286m; δ(NH_2)+ν(CH=N), 1599s; 1546m; ν(C=S), 798w. ^{1}H NMR Spectra (300MHz, δ, MeOD): δ(NH), 3.294-3.246(m, 2H); δ(Ar-H), 7.749-7.730(m, 8H); 7.413-7.392(m, 12H); δ(HC=N), 7.990(s, 4H). FAB-Mass (*m/z*): $[C_{30}H_{26}N_6S_2Zn]^{++}$ = 598.1; $[C_{23}H_{20}N_5S_2Zn]^{++}$ = 494.05; $[C_{23}H_{19}N_4S_2Zn]^{++}$ = 479.03; $[C_{18}H_{16}N_6S_2Zn]^{++}$ = 444.02; $[C_{15}H_{13}N_3SZn]^{++}$ = 331.01; $[C_{15}H_{13}N_3S]^{++}$ = 267.08; $[C_7H_7N_2]^{++}$ = 119.06; $[C_7H_6N]^{++}$ = 104.05.

*[Cd(C_6H_5CH=N-NH-CS-N=HC-C_6H_5)$_2$]Cl_2 Complex **10***

Yield: 0.230 g (32%). Mp^d=220-222 °C; Found: C, 48.39; H, 3.22; N, 10.48; S, 6.92. $C_{30}H_{26}N_6S_2Cl_2Cd$ (Mτ=718.01). Requires: C, 50.18; H, 3.64; N, 11.70; S, 8.93. Δ_m at 25 °C

($\Omega^{-1}cm^2mol^{-1}$): 179.8 in DMSO. Selected Infrared absorption (KBr, cm^{-1}): $\nu(N\text{-}H)_{asym}$, 3433m; $\nu(N\text{-}H)_{sym}$, 3272m; $\delta(NH_2)+\nu(CH=N)$, 1604s; 1554m; $\nu(C=S)$, 800w. ^1H NMR spectra (300MHz, δ, MeOD): δ(N-H), 3.345(s, H); 3.306(s, H); δ(Ar-H), 7.768-7.756(m, 8H); 7.423-7.404(m, 12H); δ(HC=N), 8.047(s, 4H). FAB-Mass (m/z): $[C_{30}H_{26}N_6S_2Cd]^{++}$ = 648.07; $[C_{23}H_{20}N_5S_2Cd]^{++}$ = 544.02; $[C_{23}H_9N_4S_2Cd]^{++}$ = 529.01; $[C_{18}H_{16}N_6S_2Cd]^{++}$ = 493.99; $[C_{15}H_{13}N_3SCd]^{++}$ = 380.99; $[C_{15}H_{13}N_3S]^{++}$ = 267.08; $[C_7H_7N_2]^{++}$ = 119.06; $[C_7H_6N]^{++}$ = 104.05. ESI-MS (*m/z*): $[C_{30}H_{26}Cl_2N_6S_2Cd^{112}]^+$ = 718.6; $[C_{30}H_{26}Cl_2N_6S_2Cd^{113}]^+$ = 719.6; $[C_{30}H_{26}Cl_2N_6S_2Cd^{114}]^+$ = 720.5.

*$[Hg(C_6H_5CH=N\text{-}NH\text{-}CS\text{-}N=HC\text{-}C_6H_5)_2]Cl_2$ Complex **12***

Yield: 0.740 g (91.9%). Mp[d]=190-195 °C. Found: C, 43.39; H, 2.88; N, 10.32; S, 6.92. $C_{30}H_{26}N_6S_2Cl_2Hg$ (Mτ=805.74). Requires: C, 44.69; H, 3.25; N, 10.42; S, 7.95. Δ_m at 25 °C ($\Omega^{-1}cm^2mol^{-1}$): 175.5 in DMSO. Selected Infrared absorption (KBr, cm^{-1}): $\nu(N\text{-}H)_{asym}$, 3414m; $\nu(N\text{-}H)_{sym}$, 3259m; $\delta(NH_2)+\nu(CH=N)$, 1600s; 1546m; $\nu(C=S)$, 808w. ^1H NMR spectra (300MHz, δ, MeOD): δ(NH), 3.321-3.284(m, 2H); δ(Ar-H), 7.742-7.733(m, 8H); 7.408-7.389(m,12H); δ(HC=N), 8.12(s, 4H). FAB-Mass (*m/z*): $[C_{30}H_{26}N_6S_2Hg]^{++}$ = 736.14; $[C_{23}H_{20}N_5S_2Hg]^{++}$ = 632.09; $[C_{23}H_{19}N_4S_2Hg]^{++}$ = 617.08; $[C_{18}H_{16}N_6S_2Hg]^{++}$ = 582.06; $[C_{15}H_{13}N_3SHg]^{++}$ = 469.05; $[C_{15}H_{13}N_3S]^{++}$ = 267.08; $[C_7H_7N_2]^{++}$ = 119.06; $[C_7H_6N]^{++}$ = 104.05.

Synthesis of nanoparticles by thermal decomposition

ZnS nanoparticles

The synthesized complex $[Zn(C_6H_5CH=N\text{-}NH\text{-}CS\text{-}NH_2)Cl_2]$/ $[Zn(C_6H_5CH=N\text{-}NH\text{-}CS\text{-}NH_2)_2]Cl_2$/ $[Zn(C_6H_5CH=N\text{-}NH\text{-}CS\text{-}N=HC\text{-}C_6H_5)Cl_2]$/ $[Zn(C_6H_5CH=N\text{-}NH\text{-}CS\text{-}N=HC\text{-}C_6H_5)_2]Cl_2$, (0.0005 mol) was mixed with triethanolamine (0.133 mL, 0.001 mol) and 10 mL of toluene in a flat bottom micro flask equipped with a glass lid. Reaction mixture was mixed thoroughly and the closed micro flask was kept in a muffle furnace at ~ 200 °C for 1 h. Thereafter, furnace was cooled till normal temperature was attained. A change in color of reaction mixture was observed and a light brown precipitate was obtained. The insoluble precipitate was washed several times by toluene, followed by methanol and then centrifuged. It was vacuum dried at room temperature. The experiments were performed at different precursor: surfactant ratio at different temperature (Table 1).

CdS nanoparticles

The synthesized complex $[Cd(C_6H_5CH=N\text{-}NH\text{-}CS\text{-}NH_2)Cl_2]$/ $[Cd(C_6H_5CH=N\text{-}NH\text{-}CS\text{-}NH_2)_2]Cl_2$/ $[Cd(C_6H_5CH=N\text{-}NH\text{-}CS\text{-}N=HC\text{-}C_6H_5)Cl_2]$/ $[Cd(C_6H_5CH=N\text{-}NH\text{-}CS\text{-}N=HC\text{-}C_6H_5)_2]Cl_2$, (0.1 mmol) was mixed with hexadecylamine (0.0241 g, 0.1 mmol) in 6 mL of toluene in a flat bottom micro flask. Reaction mixture was mixed thoroughly and the closed micro flask was kept in a muffle furnace at ~ 300 °C for 1 h. Thereafter, furnace was cooled till normal temperature was attained. A change in color was observed and a yellow precipitate was obtained. Insoluble precipitate was washed several times by toluene, followed by methanol and then centrifuged. It was vacuum dried at room temperature. The experiments were performed at different precursor: surfactant ratio at different temperature (Table 1).

HgS nanoparticles

The synthesized complex $[Hg(C_6H_5CH=N\text{-}NH\text{-}CS\text{-}NH_2)Cl_2]$/ $[Hg(C_6H_5CH=N\text{-}NH\text{-}CS\text{-}NH_2)_2]Cl_2$/ $[Hg(C_6H_5CH=N\text{-}NH\text{-}CS\text{-}N=HC\text{-}C_6H_5)Cl_2]$/ $[Hg(C_6H_5CH=N\text{-}NH\text{-}CS\text{-}N=HC\text{-}C_6H_5)_2]Cl_2$, (0.0004 mol) was mixed with Tri-octylphosphine oxide (0.773 g, 0.002 mol) in

10 mL of toluene in a flat bottom micro flask. Reaction mixture was mixed thoroughly and heated in a muffle furnace at ~200 °C for 1 h and cooled it. After cooling color of the reaction mixture was changed and a black precipitate was obtained. Insoluble precipitate was washed by toluene followed by methanol and centrifuged and then it was vacuum dried at room temperature. The experiments were performed at different precursor: surfactant ratio at different temperature (Table 1).

Table 1. Effect of precursor : surfactant ratio on the size of nanoparticles

Complex	Surfactant	Ratio of complex: surfactant	Mean particle size of nanoparticles, in nm
1, 2, 7, 8	Triethanolamine	1:1	19.2
1, 2, 7, 8	Triethanolamine	1:2	5.9
1, 2, 7, 8	Triethanolamine	1:3	5.7
1, 2, 7, 8	Triethanolamine	1:4	5.5
1, 2, 7, 8	Triethanolamine	1:5	5.2
3, 4, 9, 10	Hexadecylamine	1:1	8.5
3, 4, 9, 10	Hexadecylamine	1:2	8.3
3, 4, 9, 10	Hexadecylamine	1:3	8.2
3, 4, 9, 10	Hexadecylamine	1:4	8.0
3, 4, 9, 10	Hexadecylamine	1:5	8.0
5, 6, 11, 12	Tri-octylphosphine oxide	1:1	28
5, 6, 11, 12	Tri-octylphosphine oxide	1:2	27
5, 6, 11, 12	Tri-octylphosphine oxide	1:3	22
5, 6, 11, 12	Tri-octylphosphine oxide	1:4	17
5, 6, 11, 12	Tri-octylphosphine oxide	1:5	14

Antibacterial screening

All the metal complexes from **1-12,** the ligands 1-BTC and 1,4-DBTC and the nanoparticles of CdS, ZnS and HgS were screened for antibacterial activity against gram negative bacteria *Escherichia coli*, MTCC 1304 at different concentrations. Agar well diffusion method was used for antibacterial screening as discussed earlier[15,16]. The results in form of inhibition zone, measured in mm are presented in Table 2.

Minimum inhibitory concentration (MIC)

In order to observe the activity and confirm the sensitivity, complexes from 1-12 and nanoparticles were tested for minimum inhibitory concentration (MIC). The most popular method for MIC evaluation, commonly used in clinical laboratory is successive dilution method as discussed earlier[15-17]. MIC is concentration of the higher dilution tube, in which bacterial growth was absent and results are presented in Table 2.

Results and Discussion

Characterization of ligands

The elemental analysis data for the ligand is in good agreement with the proposed empirical formula. In FT-IR spectra of 1-BTC and 1,4-DBTC ligands two absorption bands were observed at about 1591 cm^{-1} and 1543 cm^{-1}, which may be assigned for the combination of νCH=N and aromatic ring vibrations. In the 1,4-DBTC ligand no absorption is observed in the 1620 cm^{-1} region for NH_2 deformations. It is suggested that such absorption is at a lower

frequency here, owing to the electron-withdrawing nature of the groups on the "left" of the thiocarbonyl group and mixed with ν(CH=N)[18]. Both the ligands exhibit a band at about 800 cm^{-1} assigned to (C=S).

Table 2. Antibacterial screening and MIC against *E. coli*

S. No	Complex/ligand/ nanoparticle	Activity against *E. coli*	Inhibition zone in mm	Minimum inhibitory concentration, µg/mL
A.	1-BTC	-	6	-
1.	$[ZnCl_2(1\text{-BTC})]$	+	16	34
2.	$[Zn(1\text{-BTC})_2]Cl_2$	+	18	31
3.	$[CdCl_2(1\text{-BTC})]$	+	24	37
4.	$[Cd(1\text{-BTC})_2]Cl_2$	+	32	32
5.	$[HgCl_2(1\text{-BTC})]$	+	30	32
6.	$[Hg(1\text{-BTC})_2]Cl_2$	+	34	30
B.	1,4-DBTC	-	8	-
7.	$[ZnCl_2(1,4\text{-DBTC})]$	+	17	36
8.	$[Zn(1,4\text{-DBTC})_2]Cl_2$	+	19	32
9.	$[CdCl_2(1,4\text{-DBTC})]$	+	26	36
10.	$[Cd(1,4\text{-DBTC})_2]Cl_2$	+	34	31
11.	$[HgCl_2(1,4\text{-DBTC})]$	+	32	34
12.	$[Hg(1,4\text{-DBTC})_2]Cl_2$	+	36	31
i.	ZnS nanoparticle	+	15	32
ii.	CdS nanoparticle	+	26	30
iii.	HgS nanoparticle	+	28	29
C.	Chloramphenicol	+	40	-

In ^{1}H NMR spectrum of 1-BTC two sets of multiplet between δ 7.757-7.725 ppm for 2H and δ 7.413-7.392 ppm for 3H were assigned for the aromatic protons. Two signals were observed at δ 3.315 ppm and δ 3.310 ppm for (NH) proton. The doublet at δ 3.315 ppm was assigned for (HN-C=S) group and a singlet observed at δ 3.305 ppm was attributed for (S=C-NH_2) protons of thiosemicarbazide unit. A sharp singlet observed at δ 7.89 ppm, was assigned for the CH=N proton. In ^{1}H NMR spectrum of 1, 4-DBTC two sets of multiplet between δ7.760-7.729 ppm for 4H and 7.415-7.394 ppm for 6H, were assigned for the aromatic protons. A signal observed at δ3.31 ppm, was assigned for the HN-C=S proton and a sharp singlet observed at δ7.98 ppm, was assigned for the two proton of the two (HC=N).

In FAB-mass spectra of 1-BTC the molecular ion peaks were observed at *m/z*=179, 180, and in 1, 4-DBTC, 267, 268 respectively, confirming the molecular weight of ligand to the calculated value. Thus on the basis of FT-IR, ^{1}H NMR, elemental analyses and FAB-mass spectral studies the most probable structure of the ligands were given in Figure 1 and 2.

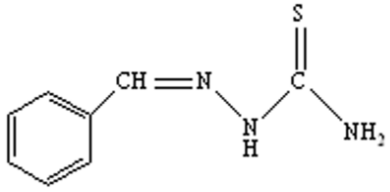

Figure 1. Structure of ligand 1-BTC

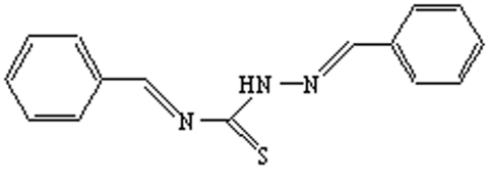

Figure 2. Structure of ligand 1,4-DBTC

Characterization of the complexes

Empirical formula of all the complexes **1-12** were in conformity with the elemental analysis. Molecular weights of all the complexes were determined by FAB-MS. A number of peaks were observed in mass spectra. Some important peaks, which were spotted in the FAB-MS of all the 1:1 complexes of 1-BTC exhibit $[MCl]^+$, $[C_8H_9ClN_3SM]^+$, $[C_8H_9Cl_2N_3SM+H]^+$. However, the 1:2 complexes of 1-BTC show $[C_{16}H_{18}ClN_6S_2M]^+$, $[C_{16}H_{18}Cl_2N_6S_2M]^+$. Similarily, the 1:1 complexes of 1,4-DBTC exhibit $[MCl]^+$, $[C_{15}H_{13}ClN_3SM]^+$, $[C_{15}H_{13}Cl_2N_3SM+H]^+$ and the 1:2 complexes show $[C_{30}H_{26}ClN_6S_2M]^+$, $[C_{30}H_{26}Cl_2N_6S_2M+H]^+$. The complex **10** was also studied by ESI-MS, which exhibit three resolved signals at 718.5, 719.5 and 720.5 were attributed for $[C_{30}H_{26}Cl_2N_6S_2Cd^{112}]^+$, $[C_{30}H_{26}Cl_2N_6S_2Cd^{113}]^+$ and $[C_{30}H_{26}Cl_2N_6S_2Cd^{114}]^+$. A representative ESI-MS spectrum of complex **10** is given in Figure 3.

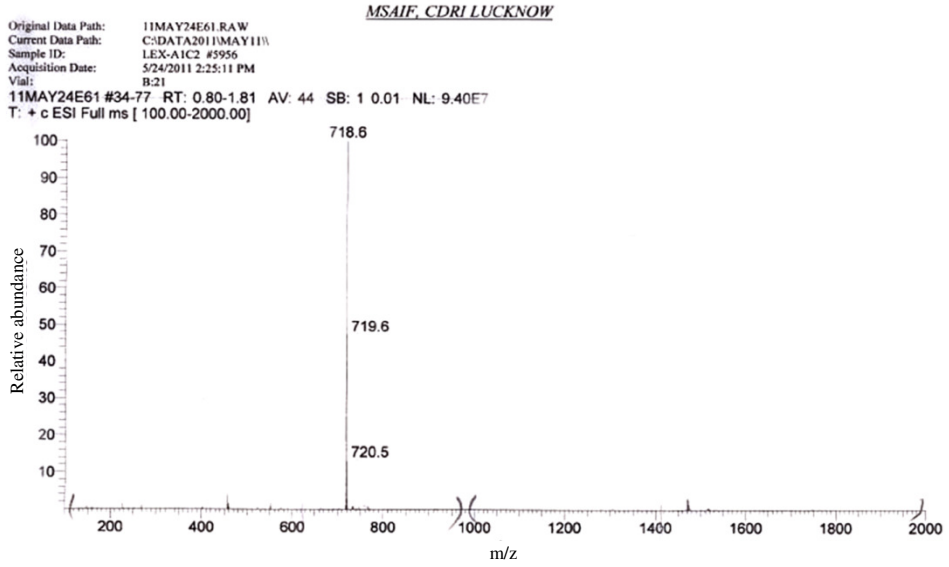

Figure 3. ESI-MS spectrum of complex 10

Molar conductance values for all the 1:1 complexes of dilute concentration (~5.0 mmol) was in the range 10-33 $\Omega^{-1}cm^2mol^{-1}$ suggesting non-electrolytic nature of the complexes. However, in the 1:2 complexes molar conductance values were quite higher and in the range 160-180 $\Omega^{-1}cm^2mol^{-1}$, indicating 1:2 electrolytic nature of the complexes.

In FTIR spectra of the ligand a sharp absorption bands exhibited at 1591 cm^{-1} and 1543 cm^{-1} in the ligand assigned for combination of ν(CH=N) and $(C=C)_{arom}$ were found shifted to higher frequency region and observed at about 1600 cm^{-1} and 1554 cm^{-1} in the complexes, indicating coordination of metal to azomethine nitrogen. A peak of medium intensity assigned for thiocarbonyl moiety was shifted in the complexes to the lower wavenumber (~35-47 cm^{-1}) inferring coordination from S of the C=S unit. A representative FTIR spectrum of complex **10** is given in Figure 4.

In ^1H NMR spectra of the complexes a signal observed at about δ7.98 ppm for the azomethine proton in ligand was shifted to lower field and appeared at about δ 8.05 ppm, indicating coordination of Schiff base ligand to metal by donating lone pair from azomethine nitrogen to the metal. In all the complexes peaks assigned for aromatic protons were observed at the same position as it was observed in their corresponding ligands. Signals for

NH and NH_2 protons were also almost unshifted in the corresponding complexes indicating nonparticipation of these groups in coordination. A representative ^{1}H NMR spectrum is given in Figure 5.

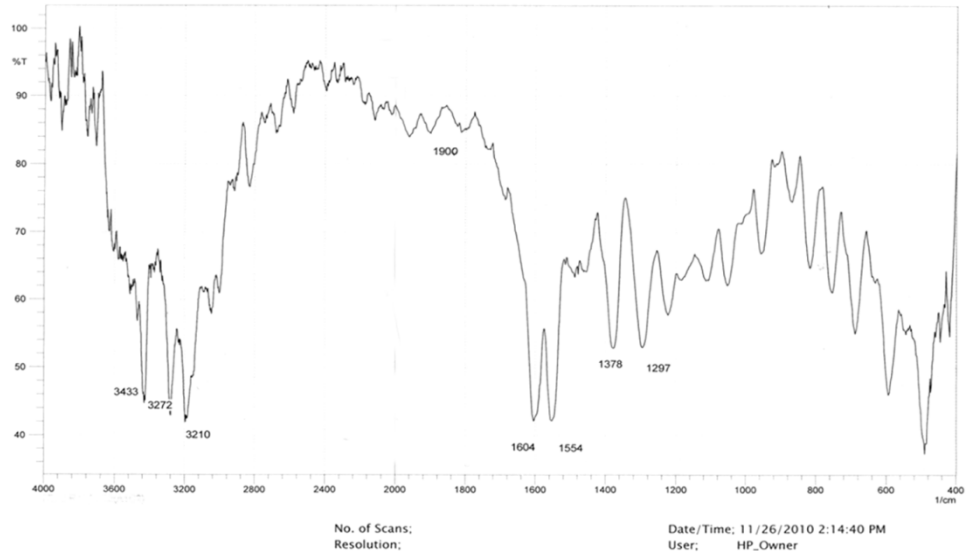

Figure 4 FT-IR spectrum of complex **10**

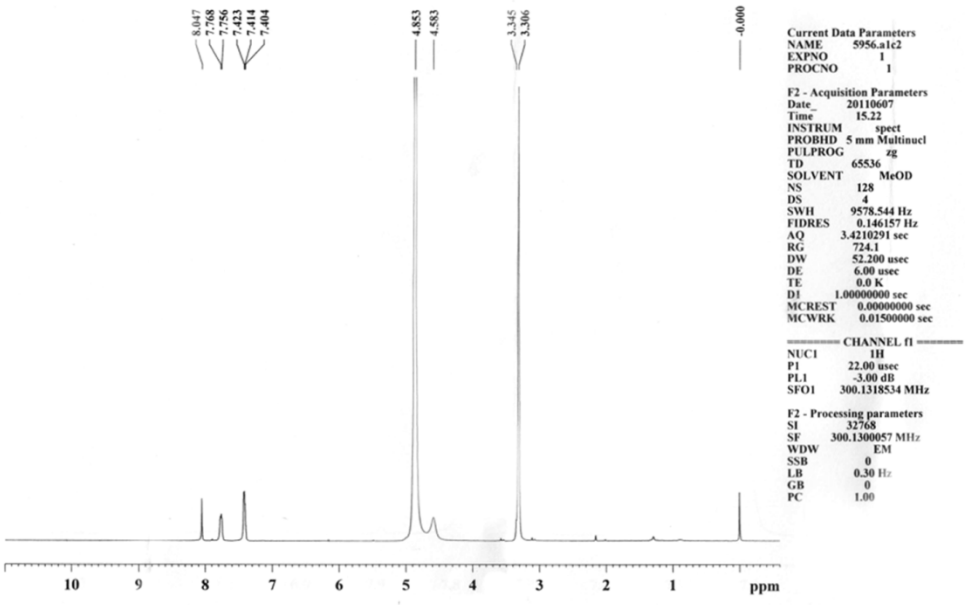

Figure 5. ^{1}H NMR spectrum of complex **10**

Therefore, on the basis of molar conductance, elemental analyses, FT-IR, ^{1}H NMR, FAB-mass and ESI-mass the most probable structure for the complexes were suggested as in Figure 6-9.

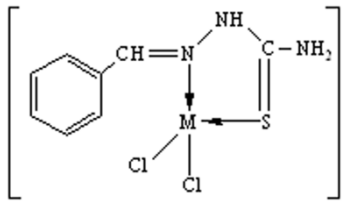

Figure 6. Complex **1, 3** and **5**

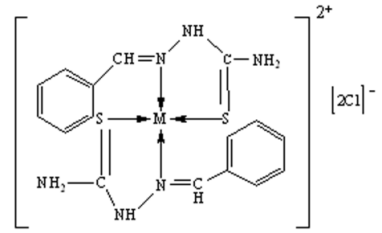

Figure 7. Complex **2, 4** and **6**

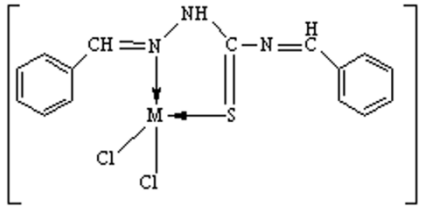

Figure 8. Complex **7, 9** and **11**

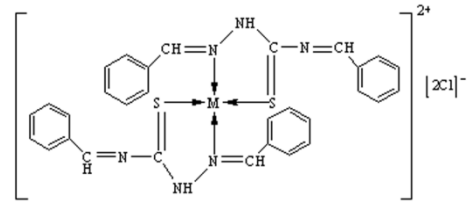

Figure 9. Complex **8, 10** and **12**

[*Where M: Zn(II), Cd(II) and Hg(II)*]

Characterization of nanoparticles

UV-Visible spectra of CdS nanoparticles

The UV-Vis spectra of CdS nanoparticles were recorded in transmission mode and samples were prepared by making dispersion in toluene. For the bulk crystallites we usually observe the inter band absorption spectrum with a band edge around 515 nm. As the crystalline size decreases there is a blue shift of the absorption edge. In the present case the band edge is observed at 406 nm with a further shoulder at about 380 nm. A similar feature for the UV-Vis spectrum of the nanocrystalline CdS has been reported by Motte and Hoyer *et al*.,[19,20].

X-Ray diffraction (XRD) measurements

XRD pattern provides information about crystalline phase of the nanoparticles as well as the crystallite size[20]. The Figure 10 shows the XRD pattern of the synthesized ZnS nanoparticles. In the XRD pattern of ZnS prominent peaks were obtained at 26.1479°, 31.9431° and 29.4394°. The calculated corresponding *d*-spacings are 3.4068, 2.7980 and 3.0326 indicating the presence of (100), (101) and (002) reflection plane and hexagonal phase. Mean crystallite size were also calculated by using Scherrer's formula[21].

The estimated average crystalline grain size of ZnS sample is 19 nm. The XRD of CdS nanoparticles (Figure 11) exhibit prominent peaks at 27.9765°, 24.6569°and 26.3167° corresponding to calculated *d*-spacing 3.1870, 3.6079 and 3.3844 respectively, indicating the presence of (101), (100) and (002) reflection planes in accordance with hexagonal phase.

The XRD of CdS also exhibit peaks at 43.5055°, 47.6409° and 51.6919° corresponding to d-spacing 2.0785, 1.9073 and 1.7669 indicating the presence of (110), (103) and (112) reflection plane also supports the existence of hexagonal phase[22]. The estimated average grain size of sample is 9.6 nm obtained from the FWHM of most intense peak.

In the XRD pattern of HgS nanoparticles (Figure 12) prominent peaks were obtained at 26.3940°, 30.5787° and 43.7234° corresponding to d-spacing 3.3740, 2.9211 and 2.0690 indicating the presence of (101), (012) and (104) reflection plane. The estimated mean grain size of the sample is 13.2 nm.

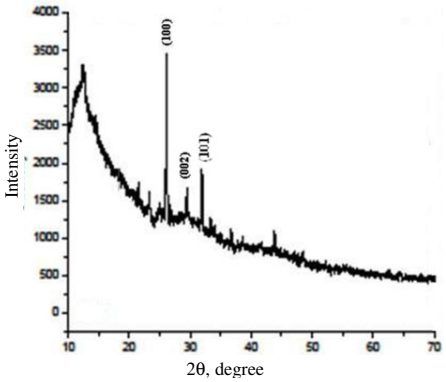

Figure 10. XRD pattern of ZnS nanoparticles

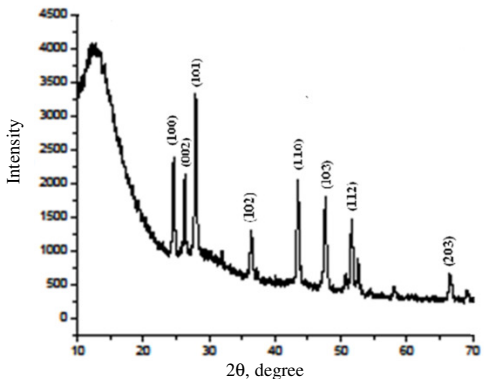

Figure 11. XRD pattern of CdS nanoparticles

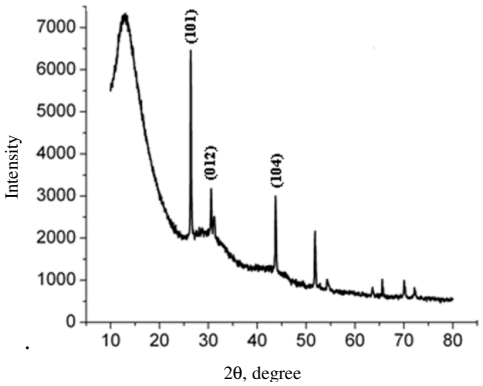

Figure 12. XRD pattern of HgS nanoparticles

Transmission electron microscopy (TEM)

TEM allows the direct imaging of nanoparticles and provides more information on the quality of individual particles, *e.g*. their size, distribution and shape[16]. The TEM image of ZnS nanoparticles (Figure 13) shows quite well-defined particles with narrow size distribution between 4.08 nm to 7.04 nm with a mean particle size of 5.9 nm (*c.f.* Table 1). The SAED of ZnS exhibits broad diffused rings that are typical of nano-sized particles and a representative pattern is shown in Figure 14. The *d*-spacing values calculated from the SAED pattern are 3.3500, 3.3444 and 2.1097, which are in a good agreement with the XRD results. The size distribution graph is shown in Figure 15.

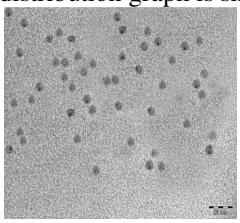

Figure 13. TEM image of ZnS nanoparticles

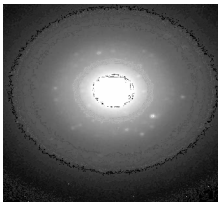

Figure 14. SAED pattern of ZnS nanoparticles

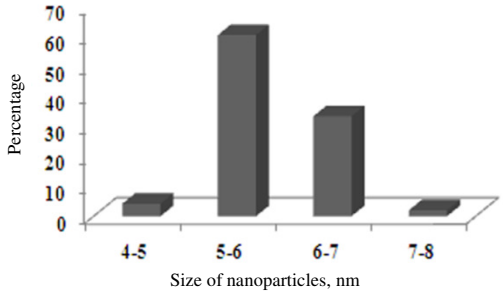

Figure 15. Distribution graph of different size of ZnS nanoparticles

The TEM image of CdS nanoparticles (Figure 16) shows quite well defined hexagonal particles with a narrow size distribution from 5.32 nm to 13.11 nm and mean particle size 8.5 nm (*c.f.* Table 1), indicating very good correlation with XRD results. The SAED of CdS exhibits broad diffused rings that are typical of nano-sized particles and a representative pattern is shown in Figure 17. The d-spacing values calculated from the SAED pattern are 3.3112, 2.0920 and 1.7809, which are in a good agreement with the XRD results. The size distribution graph is shown in Figure 18.

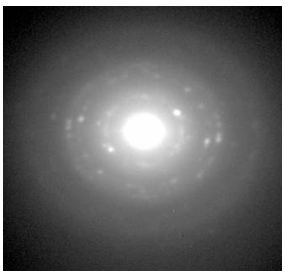

Figure 16. TEM image of CdS nanoparticles

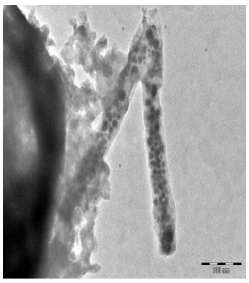

Figure 17. SAED pattern of CdS nanoparticles

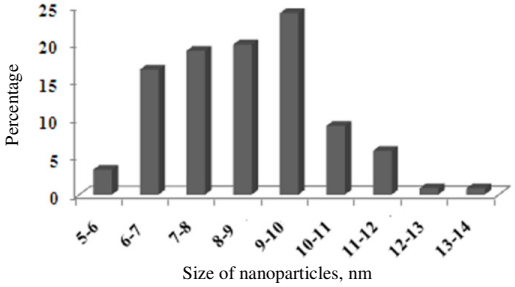

Figure 18. Distribution graph of different size of CdS nanoparticles

The TEM image of HgS nanoparticles (Figure 19) shows quite well defined hexagonal particles with a narrow size distribution from 9.09 nm to 23.86 nm and mean particle size 14 nm (*c.f.* Table 1), indicating a very good correlation with XRD results. The SAED of HgS exhibits broad diffused rings that are typical of nano-sized particles and a representative pattern is shown in Figure 20. The d-spacing values calculated from the SAED pattern are 3.4662, 2.1097 and 1.7953, which are in a good agreement with the XRD results. The size distribution graph is shown in Figure 21.

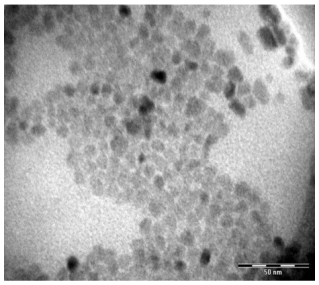

Figure 19. TEM image of HgS nanoparticles

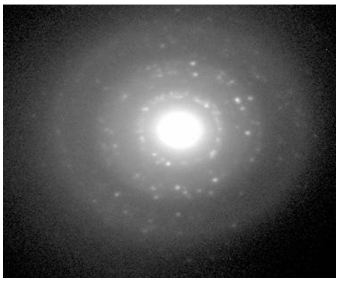

Figure 20. SAED pattern of HgS nanoparticles

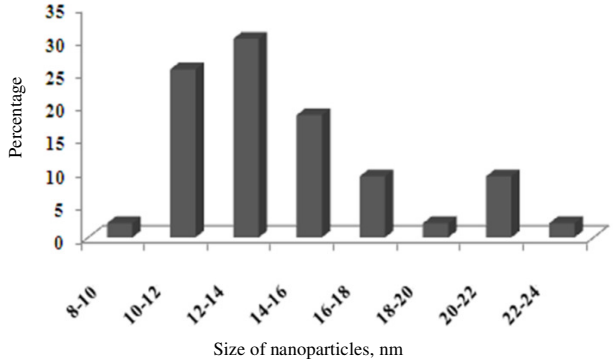

Figure 21 Distribution graph of different size of HgS nanoparticles.

Antibacterial activity

It was observed that all the metal complexes show much more activity in comparison to the Schiff base, probably due to enhanced lipophilicity of the complexes, which leads to the breakdown of permeability barrier of the cell and thus retards the normal cell process in bacteria. It is postulated that improved activity arises from the delocalization of positive charge between the organic moiety and the metal, which favours the drug entering into normal cellular processes of the bacteria. The increased activity of metal complexes can also be explained on the basis of '*Overtone's concept*' and '*Chelation theory*'[16].

Minimum inhibitory concentration (MIC)

It was observed that the complex **12** was the most active to inhibit bacteria with inhibition zone of **36** mm but the complex **6** has lowest minimum inhibitory concentration of 0.30 µg/mL for *E. coli*. Mercuric sulphide nanoparticles have even more lower MIC value of 0.29 µg/mL. However, it was interestingly observed that activity of all the complexes decreases with dilution but in nanoparticles activity was observed same even at more dilution, which may be attributed to the increased ratio of surface area to volume in the nanoparticles.

Conclusion

Twelve complexes of Zn(II), Cd(II) and Hg(II) with two Schiff base ligands 1-benzylidene thiosemicarbazide and 1,4-dibenzylidene thiosemicarbazide have been synthesized and characterized by spectroscopic methods. The complexes along with surfactant in the ratio ranging between 1:1 to 1:5 for precursor: surfactant, were used as single source precursor for the thermal/ pyrolytic synthesis of ZnS, CdS and HgS nanoparticles. Interestingly, it was

observed that, at low concentration of precursor and high concentration of surfactant the nanoparticles are hexagonal in shape and smaller in size. In synthesis of HgS nanoparticles 1:5, precursor : surfactant ratio is most favourable and in TEM pictures nanoparticles are found entrenched in finger like surroundings probably due to high concentration of surfactant (*c.f.* Table 1). At high temperature agglomeration takes place and large particle size are favoured. In this work Schiff base complexes were probably for the first time used as single source precursor for the synthesis of metal sulphide nanoparticles. All the complexes were screened for antibacterial activity against *E. coli* and found more potent than the corresponding Schiff base ligands and exhibit approximately same toxicity as standard drug. However, nanoparticles exhibited more antibacterial activity than the Schiff bases but less than the complexes. It can be concluded that nanoparticles exhibited potency due to their greater surface area, but the synergistic effect of toxophoric functions are more prominent in the complexes, due to which probably the complexes are more potent than nanoparticles. Interestingly, nanoparticles exhibit lower MIC than the complexes probably due to their higher surface activity.

Acknowledgement

We are thankful to our Principal, Govt. Model Science College, Jabalpur and Head, Department of Chemistry, Govt. Model Science College, Jabalpur(M.P.) India for providing laboratory facilities. One of us (SNS) is thankful to UGC for the sanction of Major Research Project F No.39-839/2010(SR). We are indebted to Dr. Mukul Gupta Scientist-E, DAE-UGC Consortium Research Center, Indore for his kind help rendered in XRD measurements. We are also thankful to Dr. N. P. Lalla, Scientist-F, DAE-UGC Consortium Research Center, Indore for his kind help in TEM Measurements. Thanks are also due to SAIF, CDRI, Lucknow for CHNS analyses, ^{1}H NMR and ESI-MS/FAB-MS spectra.

References

1. Chen J, Saeki F, Wileym B J, Cang H, Cobb M_J, Li Z_Y, Au L, Zhang H, Kimmey M_B, Li X and Xia Y. *Nano Lett.,* 2005, **5(3)**, 473-477; DOI:10.1021/nl047950t
2. Gobin A M, Lee M H, Halas N J, James W D and Drezek R A *Nano Lett.,* 2007, **7(7)**, 1929-1934; DOI:10.1021/nl070610y
3. Fu A, Gu W, Boussert B, Kristie Koski, Daniele Gerion, Liberato Manna, Mark Le Gros, Carolyn A. Larabell and Paul Alivisatos A, *Nano Lett.,* 2007, **7(1)**, 179-182; DOI:10.1021/nl0626434
4. Zhao H, Douglas E P, Harrison B S and Schance K S, *Langmuir,* 2001, **17(26)**, 8428-8433; DOI:10.1021/la011348q
5. Madarasz J, Bombicz P, Okuya M and Kaneko S, *Solid State Ionics,* 2001, **141-142**, 439-446; DOI:10.1016/S0167-2738(01)00740-8
6. Zhai C, Zhang H, Du N, Chen B, Huang H, Wu Y and Yang D, *Nanoscale Res Lett.,* 2011, **6**, 31-35.
7. Dong X Y, Mi X N, Zhao W W, Xu J J and Chen H Y, *Biosens Bioelectron,* 2011, **26(8)**, 3654-3659; DOI:10.1016/j.bios.2011.02.023
8. Shiohara A, Hoshino A, Hanaki K, Suzuki K and Yamamoto K *Microbiology Immunology,* 2004, **48(9)**, 669-675; DOI:10.1111/j.1348-0421.2004.tb03478.x
9. Shukla S N, Gaur P. Rai N and Mehrotra R, *J Chinese Chem Soc.,* 2014, **61(5),** 594-604; DOI:10.1002/jccs.201300454
10. Greer A H and Smith G B L, *J Am Chem.Soc.*, 1950, **72(2)**, 874-875; DOI:10.1021/ja01158a059

11. Bernstein J, Lott W A and Wiselogle F Y, *U. S. Patent,* 1953, **635(2)**, 115.
12. Lieber E and Ramchandran P, *Can J Chem.,* 1959, **37(1)**, 101-109; DOI:10.1139/v59-015
13. Jensen K A, *J Prakt Chem.,* 1941, **159**, 189-192.
14. Traverso G, *Gazz Chim Ital.,* 1953, **83**, 1027.
15. Pelczar M J, Chan E C S and Krieg N R, Text Book of Microbiology; 5th Ed.; McGraw-Hill Publishing Company Ltd.; New Delhi, India, 2001, pp 138.
16. Shukla S N, Gaur P and Rai N, *Appl Nanosci.,* 2015, **5(5)**, 583-593; DOI:10.1007/s13204-014-0351-0
17. Mazzola P G, Jozala A F, Novaes L C L, Moriel P and Penna T C V, *Braz J Pharma* Sci., 2009, **45(2)**, 241-248.
18. Wiles D M and Suprunchuk T, *Can J Chem.,* 1969, **47**, 1087.
19. Motte L, Petit C, Boulanger L, Lixon P and Pileni M P, *Langmuir,* 1992, **8**, 1049-1053; DOI:10.1021/la00040a006
20. Hoyer P, Baba N and Masuda H, *Appl Phys Lett.,* 1995, **66(20)**, 2700-2702; DOI:10.1063/1.113493
21. Nair P S, Radhakrishnan T, Revaprasadu N, Kolawole G and O'Brien P, *J Mater Chem.,* 2002, **12**, 2722-2725; DOI:10.1039/B202072F
22. Manickathai K, Viswanathan S K and Alagar M, *Ind J Pure Appl Phy.,* 2008, **46** 561-564.